



## Materials

The BPM head will be made of non-magnetic materials to avoid magnetic interference with adjacent quadrupole and sextupole magnetic fields. We selected stainless steel (316L) as a material of the water-cooled BPM block welded to the vacuum chamber made of the same stainless steel. The material of the outer flange of the electrode welded to the block is also stainless steel (316L). To suppress the heating of the button and center pin of the electrode thermally connected to the block only through the insulator of alumina ceramic, as their material, we have selected molybdenum (Mo) with high electric and thermal conductivities which are nearly ten-times larger than that of stainless steel or titanium. Molybdenum also suits for high-accuracy machining.

## Mechanical Tolerance

To satisfy the error budget defined for the BPM offset of 100  $\mu\text{m}$  rms, we have specified machining tolerances of the button electrode (Fig. 2) and its mounting hole of the BPM block. The tolerances of the button diameter and the vertical mounting position in the BPM block are specified as  $\pm 30 \mu\text{m}$  and 50  $\mu\text{m}$  as an offset back into the hole, respectively. To ensure the horizontal position accuracy of the button, we have specified the concentricity of 50  $\mu\text{m}$  between the button and the outer flange of the electrode which fits in the housing hole of the BPM block.

## RF AND THERMAL SIMULATIONS

The results of simulation studies for the design optimization are summarized in this section. The RF characteristics (beam signals, beam coupling impedances and trapped modes) were calculated using CST STUDIO SUITE [6] and the thermal issues were analysed using ANSYS [7].

### Ohmic Loss Minimization

Trapped resonance modes excited in a coaxial structure of the BPM electrode lead to heating and beam coupling impedance. The dominant resonance modes contributing to loss factor  $\kappa_{loss}$  coming from the beam impedance are excited in a gap between the button and the housing hole as shown in the next section (Fig. 5). Therefore, the geometric dimensions relevant to the strength of the main trapped mode resonances are the size of the gap and the button thickness. Narrowing the gap simply reduces the resonance strengths, though, it requires tighter machining tolerance to avoid electric short between the button and the housing hole. We selected the same gap of 0.5 mm as the BPM button of the present SPring-8, since we have experienced no troubles with the electric short or discharge. The button thickness was optimized to minimize the ohmic loss. The total ohmic loss  $P_{loss}$  of a BPM head including loss in four electrodes and wall loss is expressed by,

$$P_{loss} = \kappa_{loss}(\sigma_t) \frac{Q_b^2}{T_b} - 4P_{sig}, \quad (1)$$

where  $Q_b$ ,  $T_b$  and  $P_{sig}$  are bunch charge, bunch spacing and output signal power per button electrode, respectively.

The loss factor  $\kappa_{loss}$  in frequency domain is defined by

$$\kappa_{loss}(\sigma_t) = \frac{1}{2\pi} \int_0^\infty h(\omega; \sigma_t) d\omega. \quad (2)$$

The function  $h(\omega, \sigma_t)$  is the longitudinal impedance of a BPM head weighted with a power spectrum of a bunched beam,

$$h(\omega; \sigma_t) = 2\text{Re}[Z_{||}(\omega)] e^{-\omega^2 \sigma_t^2}. \quad (3)$$

Here,  $Z_{||}$  and  $\sigma_t$  are longitudinal impedance and bunch length (rms), respectively. Figure 3 shows the total ohmic loss as a function of the button thickness for a temporary bunch fill pattern of 0.25 mA/bunch\*406 which gave the maximum heat load among the equally spaced bunch fill patterns for a total stored current of 100 mA. In the calculation, bunch lengthening due to potential well distortion was taken into account by a preliminary beam impedance model for the whole of the new ring. Here, the bunch length  $\sigma_t$  is evaluated to be 14 ps for the bunch current of 0.25 mA. We selected a button thicknesses of 5 mm giving the minimum ohmic loss in the calculation.

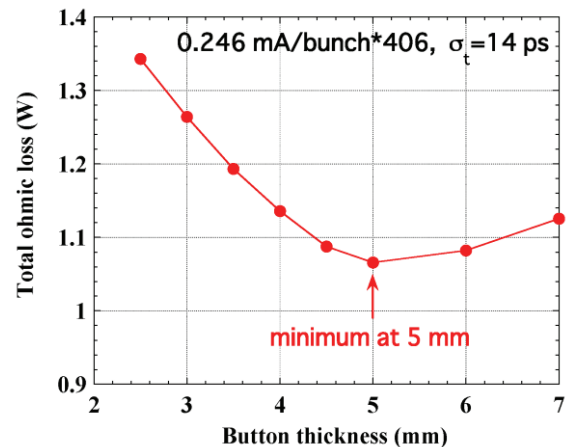


Figure 3: The total ohmic loss of a BPM head as a function of the button thickness calculated for a temporary bunch fill pattern of 0.25 mA/bunch\*406 with a total stored current of 100 mA (see text).

### Trapped Modes Analysis

The frequency spectrum of the trapped resonance modes is given by  $h(\omega, \sigma_t)$  of Eq. (3). Figure 4 shows the function  $h(\omega, \sigma_t)$  calculated for the BPM head with the optimized electrodes. The diameter and height of the button are  $\phi 7$  mm and 5 mm, respectively. The bunch length of 14 ps (rms) is assumed.

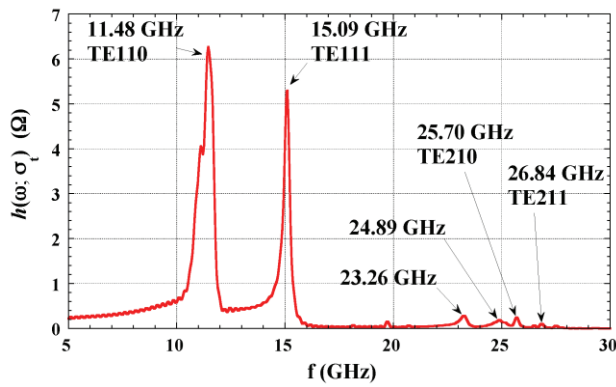


Figure 4: Calculated frequency spectrum of the trapped resonance modes (see text).

Two resonance peaks at the frequencies of 11.48 and 15.09 GHz stand for the main trapped modes. Some weak resonance modes are also excited in the frequency range from 20 to 30 GHz. We computed the electro-magnetic fields distributions of each mode at the resonance peak frequencies. Figure 5 shows the distributions of magnetic fields, which can cause heating of the BPM electrode and the block. The trapped modes classified as TE-modes by the computed field distributions are excited in the gaps of 0.5 mm between the buttons and the housing holes for the electrodes. The weak resonance modes at 23.26 and 24.89 GHz are also excited in the ceramic around the center pin.

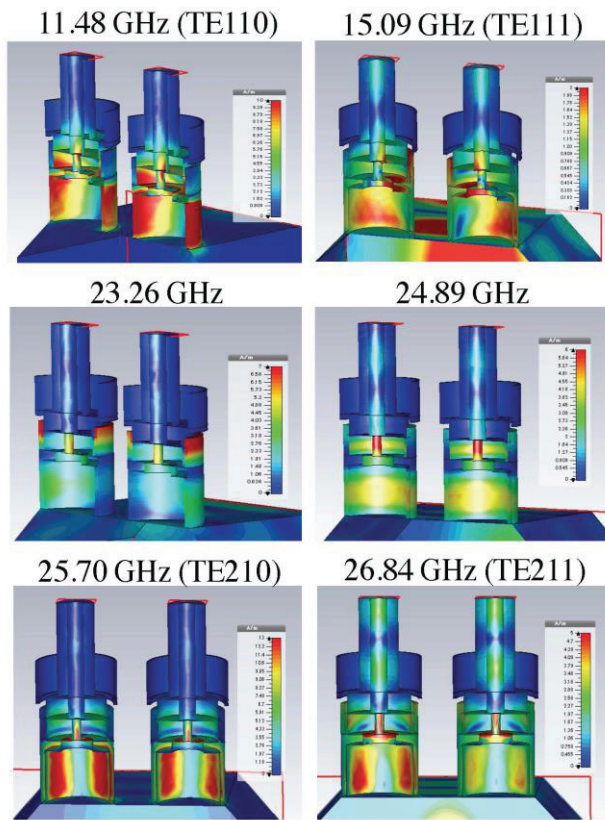


Figure 5: Computed magnetic field distributions of the trapped modes at the resonance frequencies in Fig. 4.

### Heating of the BPM Electrode and the Block

It is important to evaluate the trapped mode heating of the BPM electrode and its housing hole, and the wall current heating of the BPM block. Thermal deformations of the button and the block could cause a drift of the BPM offset, which deteriorates the long-term stability of the BPM system. The BPM block is water-cooled to remove the heat dissipated in the electrodes and their housing holes, and the heat by wall current loss. To evaluate the heat input to each part of the electrode (the button, center pin) and the inside of the housing hole, we calculated the contribution to the loss factor of each trapped mode by integrating the resonance peak corresponding to each mode shown in Fig. 4. Here, the contribution of the wall current loss is subtracted from the integrals. The heat input to each part is given by the sum of the integrated ohmic losses of the relevant trapped modes. Figure 6 shows the evaluated heat input to the molybdenum button side, center pin, inside of the housing hole of the stainless steel BPM block, and the flat-tops of the beam pipe inside the block. The temporary bunch fill pattern of 0.25 mA/bunch\*406 with the bunch length of 14 ps is assumed. The total heat input evaluated for the whole of the BPM head is 1.1 W. We have computed the temperature distribution of the BPM head with the heat input condition shown in Fig. 6. The temperature of the cooling water for the BPM block is set at 30 °C, and its flow velocity in the cooling channel with 6 mm diameter is 0.6 m/s. The heat transfer coefficient from the block to the cooling water is calculated to be 4300 W/m<sup>2</sup>/K for turbulent flow condition. The natural heat dissipation to the surrounding air of 27 °C is also taken into account with the heat transfer coefficient of 5 W/m<sup>2</sup>/K. The heat generated at the molybdenum button and center pin is transferred to the water-cooled block through the alumina ceramic with thermal conductivity of 18 W/m/K which is close to that of stainless steel. The computed temperature distribution is shown in Fig. 7. The maximum temperature obtained in the calculation is 31 °C on the button surface.

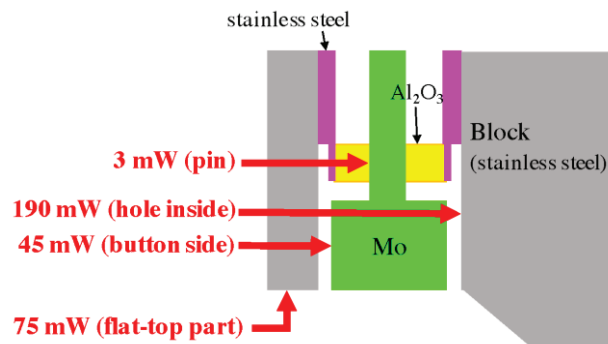


Figure 6: The heat input model for thermal simulation of the BPM electrode and the BPM block (see text).

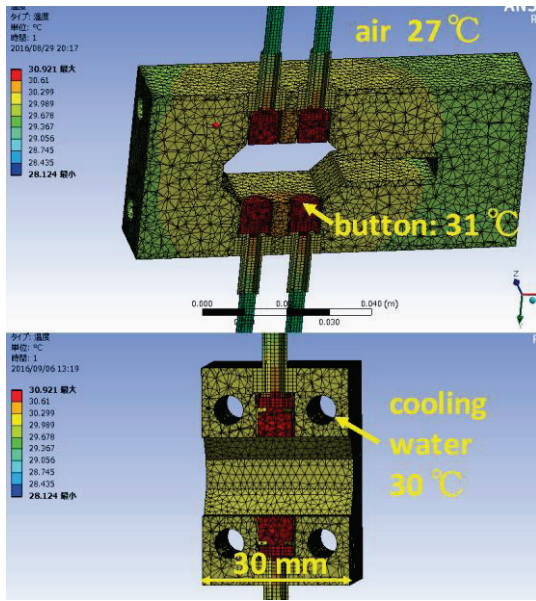


Figure 7: Computed temperature distribution of the BPM head. Maximum temperature is 31 °C on the button of the electrode.

### Signal Intensity

In the vicinity of the center of a BPM, a beam position  $(x_b, y_b)$  is calculated by

$$(x_b, y_b) = \left( k_x \frac{V_1 - V_2 - V_3 + V_4}{V_1 + V_2 + V_3 + V_4}, k_y \frac{V_1 + V_2 - V_3 - V_4}{V_1 + V_2 + V_3 + V_4} \right), \quad (4)$$

where  $V_1, V_2, V_3, V_4$  are the signal intensities from the four button electrodes. For the designed BPM electrode (Fig. 2) and BPM block (Fig. 1), the horizontal and vertical sensitivity coefficients ( $k_x, k_y$ ) are calculated to be (6.8 mm, 7.7 mm). The beam signal voltage  $V$  for satisfying the demanded position resolution  $\sigma_{resol}$  is given by

$$V > \frac{k_{x,y}}{2\sigma_{resol}} \sigma_V, \quad (5)$$

where  $\sigma_V$  is the signal voltage fluctuation due to thermal and electric noises. The thermal noise power at an input to a signal processor circuit is estimated to be -101 dBm for the bandwidth of 10 MHz at the room temperature of 300 K. When the noise figure of a processor is assumed to be 14 dB including cable loss for the original designed circuit [3] as one of the candidates of BPM electronics for the SPring-8 upgrade, the equivalent input noise power is -87 dBm, that is corresponding to the signal voltage fluctuation  $\sigma_V$  of 10  $\mu$ V. From Eq. (5) with the vertical sensitivity coefficient  $k_y$  of 7.7 mm, we can calculate the signal voltage of 0.38 mV or power of -55 dBm required for the resolution  $\sigma_{resol}$  of 100  $\mu$ m. For the SP measurement of a single bunch beam of 100 pC charge, the signal power spectrum with 10 MHz bandwidth calculated for the designed  $\phi 7 \times 5$  mm button electrode is shown in Fig. 8. The signal intensity at the detection frequency of the processor circuit, same as the RF frequency of 508.76 MHz, is -53 dBm larger than the requirement.

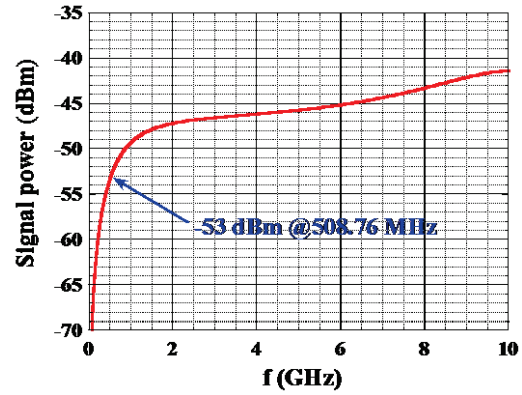


Figure 8: Calculated power spectrum of the BPM output signal in 10 MHz bandwidth for a 100 pC single bunch.

### SUMMARY

We have designed and developed the button-type BPM electrodes for the SPring-8 upgrade. The mechanical structure and the tolerances, and the materials are optimized to maximize the signal intensity, to satisfy the allowable BPM offset error, and to minimize the trapped mode heating of the electrode. Manufacturing of the prototypes of the designed electrode is in progress. We have a plan for a beam test of the prototypes at the present SPring-8 storage ring. The performance of the designed BPM electrode (the signal intensity, the signal waveform, and the heating by electron beam) will be verified.

### ACKNOWLEDGEMENT

Authors would like to thank B. K. Scheidt for useful comments and discussions on the materials for the button electrode.

### REFERENCES

- [1] SPring-8-II Conceptual Design Report, Nov. 2014, <http://rsc.riken.jp/pdf/SPring-8-II.pdf>
- [2] H. Tanaka, *et al.*, “SPring-8 Upgrade Project”, in Proceedings of IPAC2016, Busan, Korea, May 2016, WEPOW019, pp. 2867-2870.
- [3] H. Maesaka, *et al.*, “Development Status of a Stable BPMSystem for the SPring-8 Upgrade”, presented at IBIC2016, Barcelona, Spain, Sep. 2016, TUPG06, this conference.
- [4] M. Oishi, *et al.*, “Design and R&D for the SPring-8 Upgrade Storage Ring Vacuum System”, in Proceedings of IPAC2016, Busan, Korea, May 2016, THPMY001, pp.3651-3653.
- [5] T. Watanabe, *et al.*, “Magnet Development for SPring-8 Upgrade”, in Proceedings of IPAC2016, Busan, Korea, May 2016, TUOCB03, pp.1093-1095.
- [6] CST STUDIO SUITE, <http://www.cst.com/>
- [7] ANSYS, <http://www.ansys.com/>